

Northumbria Research Link

Citation: Mukhopadhyay, Tanmoy, Ma, Jiayao, Feng, Huijuan, Hou, Degao, Gattas, Joseph M., Chen, Yan and You, Zhong (2020) Programmable stiffness and shape modulation in origami materials: Emergence of a distant actuation feature. *Applied Materials Today*, 19. p. 100537. ISSN 2352-9407

Published by: Elsevier

URL: <https://doi.org/10.1016/j.apmt.2019.100537>
<<https://doi.org/10.1016/j.apmt.2019.100537>>

This version was downloaded from Northumbria Research Link:
<http://nrl.northumbria.ac.uk/id/eprint/43930/>

Northumbria University has developed Northumbria Research Link (NRL) to enable users to access the University's research output. Copyright © and moral rights for items on NRL are retained by the individual author(s) and/or other copyright owners. Single copies of full items can be reproduced, displayed or performed, and given to third parties in any format or medium for personal research or study, educational, or not-for-profit purposes without prior permission or charge, provided the authors, title and full bibliographic details are given, as well as a hyperlink and/or URL to the original metadata page. The content must not be changed in any way. Full items must not be sold commercially in any format or medium without formal permission of the copyright holder. The full policy is available online: <http://nrl.northumbria.ac.uk/policies.html>

This document may differ from the final, published version of the research and has been made available online in accordance with publisher policies. To read and/or cite from the published version of the research, please visit the publisher's website (a subscription may be required.)

Programmable stiffness and shape modulation in origami materials: Emergence of a distant actuation feature

Tanmoy Mukhopadhyay^{1*}, Jiayao Ma^{2,3*}, Huijuan Feng^{2,3}, Degao Hou^{2,3}, Joseph M. Gattas⁴, Yan Chen^{2,3§},
Zhong You^{1,3§}

AUTHOR AFFILIATIONS

¹ Department of Engineering Science, University of Oxford, Parks Road, Oxford, OX1 3PJ, UK

² Key Laboratory of Mechanism Theory and Equipment Design of Ministry of Education, Tianjin University, Tianjin 300072, China

³ School of Mechanical Engineering, Tianjin University, Tianjin 300072, China

⁴ School of Civil Engineering, University of Queensland, St. Lucia, Australia

* Joint first authors

§ To whom correspondence should be addressed. Email: yan_chen@tju.edu.cn (YC), zhong.you@eng.ox.ac.uk (ZY)

Abstract

This paper develops an origami based mechanical metamaterial with programmable deformation-dependent stiffness and shape modulation, leading to the realization of a distant actuation feature. Through computational and experimental analyses, we have uncovered that a waterbomb based tubular metamaterial can undergo mixed mode of deformations involving both rigid origami motion and structural deformation. Besides the capability of achieving a near-zero stiffness, a contact phase is identified that initiates a substantial increase in the stiffness with programmable features during deformation of the metamaterial. Initiation of the contact phase as a function of the applied global load can be designed based on the microstructural geometry of the waterbomb bases and their assembly. The tubular metamaterial can exhibit a unique deformation dependent spatially varying mixed mode Poisson's ratio, which is achievable from a uniform initial configuration of the metamaterial. The spatial profile of the metamaterial can be modulated as a function of the applied far-field global force, and the configuration and assembly of the waterbomb bases. This creates a new possibility of developing a distant actuation feature in the metamaterial enabling us to achieve controlled local actuation through the application of a single far-field force. The distant actuation feature eliminates the need of installing embedded complex network of sensors, actuators and controllers in the material. The fundamental programmable features of the origami metamaterial unravelled in this paper can find wide range of applications in soft robotics, aerospace, biomedical devices and various other advanced physical systems.

Keywords

Programmable mechanical metamaterial; Extreme stiffness modulation; Microstructure-dependent shape modulation; Distant actuation; Waterbomb origami

1. Introduction

Natural and engineered materials have taken a crucial role in the history of human civilization; mechanical metamaterials are among the major defining materials in the current era with extraordinary promises of applicability in a number of high-end engineering and physical systems. Their mechanical attributes can be tailored to specific engineering demands leading to extreme and unusual (not achievable in conventional materials), yet useful properties, resulting in a range of benefits for various multi-functional systems [1]. Such mechanical metamaterials are developed by artificially designing multi-functional microstructures for achieving application-specific multi-objective goals, wherein the mechanical properties at the global macro-scale are defined by the structural and geometric configurations at the microscale rather than only intrinsic material properties of the constituent members [2 – 5]. Recently origami objects have become popular candidates in the design of mechanical metamaterials with a programmable stiffness that is adaptive and responsive to the external loading and boundary conditions as well as physical environment they operate in. Typically an origami based metamaterial is created by stacking a series of foldable origami patterns, each of which is formed by the repetitive tessellation of origami units [6 – 9]. For a given origami pattern, the variation of the stiffness of such a material with the change in geometric dimensions is well-documented. It has also been reported that a sharp alteration (increase) in stiffness can be achieved by distortion of some basic origami units, e.g., by a forced inversion of one or a number of vertices [10 – 11]. However, such a distortion changes the fundamental nature of an origami pattern, which may render it unrecoverable, resulting in problems such as consistency and repeatability under a cyclic loading. Here we aim to report a waterbomb origami based tubular material microstructure that can exhibit a range of unique, yet useful mechanical features suitable for various prospective structural applications. The metamaterial has an *inherent* ability to change seamlessly from purely rigid origami morphing to deformable structural behaviour while being compressed, resulting in a steep increase in its stiffness. Its shape can be modulated by a far-field force, leading to distant actuation of local behaviours. These unique properties make it an ideal candidate for developing a self-tuneable metamaterial that can be programmed according to application-specific requirements.

Tubular metamaterials are receiving increased attention from the scientific community in recent years due to the exciting mechanical and electronic properties such as vibro-acoustic modulation [12], non-volatile mechanical memory operation [13], stiffness and shape modulation [8, 14]. Here the waterbomb tube refers to an origami based metamaterial obtained by tessellation of waterbomb bases (refer to Fig. 1), typically which comprise of four diagonal valley creases and two co-linear mountain creases all meeting at a single vertex at the middle [15 – 18]. An intriguing feature of the waterbomb tube is that it can exhibit negative Poisson's ratio, i.e. both of its length

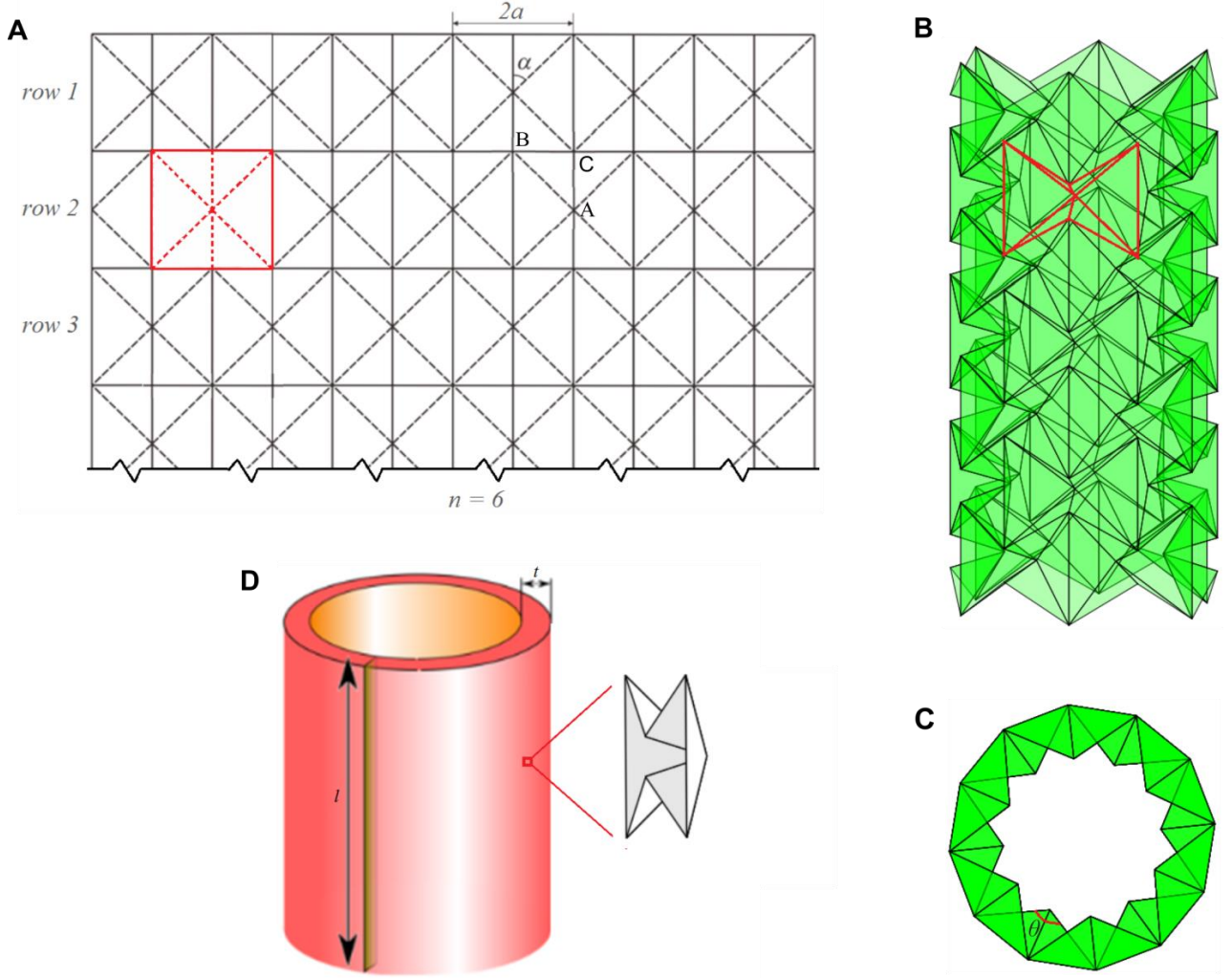


Figure 1. The waterbomb origami pattern and model. **A.** The waterbomb pattern formed by tessellating the waterbomb bases. Solid and dashed lines represent mountain and valley creases, respectively. A typical base is shown in red, which are placed side-by-side forming a row. On the adjacent rows, the bases are shifted by half a base. Four geometrical parameters — width of the base $2a$, angle α , the numbers of bases in the vertical direction, m , and horizontal direction, n — completely define the pattern. A, B and C are three representative vertices. **B.** Three dimensional view of a waterbomb tube obtained from the base pattern shown in Figure 1A. A typical waterbomb unit is highlighted in red colour. **C.** Top view of the waterbomb tube. Here the dihedral angle θ is the angle between two largest facets of a waterbomb unit. **D.** An idealized representation of the tubular meta-structure at macro scale where the constituting units are made of waterbomb based microstructure as shown in a zoomed format.

and radius get smaller under compressive load, and vice-versa [19]. This feature has been utilized in a range of practical applications including expandable medical stent graft [19, 20], transformable worm robot [21] and deformable robot wheel [22]. Despite few such applications, the precise motion behaviour and mechanical properties of waterbomb tubes have remained ambiguous and vastly unexplored. These aspects are central to the waterbomb based tubular system for creating a metamaterial and for a range of other current and future applications. If the folding is purely rigid as

other rigid origami patterns such as Miura-ori (no facet deformation), one needs to only focus on engineering the creases that undergo large rotations [7, 8]. If, however, the motion is non-rigid, both creases and facets would have to be suitably designed to withstand a certain amount of deformation [10, 11]. Such complex behaviour could lead to interesting exploitable dimensions in the mechanical properties of microstructured materials. Therefore, in this article, we aim to uncover the mechanical behaviour and constitutive relations of the waterbomb tube metamaterial through detailed physics-based simulations and physical experiments.

2. Results

Here we present detailed geometry of the waterbomb based tubular metamaterial describing the underlying parameters for modulating mechanical properties of the structural system. The crease pattern of a waterbomb based tubular metamaterial is depicted in Fig. 1A, where the pattern has three distinct vertex groups: central vertices A, and edge vertices B and C. A tubular form (refer to Fig. 1B) can be obtained when the left and right edges of the pattern are joined together. The metamaterial, as constructed from the pattern shown in Fig. 1A, can be defined by four independent geometric parameters — width $2a$, angle α , and the number of bases longitudinally, m , and circumferentially, n . An idealized representation of the tubular meta-structure at macro scale is shown in Fig. 1D, wherein the constituting units are made of waterbomb based microstructure as shown in a zoomed format.

A representative physical model can best explain the behaviour of the waterbomb tube. First, we create a waterbomb tube of uniform radius with seven rows as shown in Fig. 2A. When the tube contracts slightly along its longitudinal axis, both its radius and length reduce exhibiting a negative Poisson's ratio (refer to Fig. 2A(II)). With further contraction, the tube develops a pineapple shape (refer to Fig. 2A(III)), and subsequently the tube regains uniform radius as shown in Fig. 2A(IV). This is followed by shrinkage in radius at the equatorial row (i.e. the middle row) of the tube as depicted in Fig. 2A(V). On the basis of the physical model, the following observations can be made; that also become evident from the subsequent numerical results. First, all of the waterbomb units in the same row, placed side-by-side circumferentially at any stage of deformation, behave in an identical manner. Second, each individual base remains plane-symmetric (i.e. symmetric about the plane formed by two mid-mountain creases; this plane also passes through the longitudinal axis of the tube) during the deformation. At all stages of deformation, the top and bottom halves of the tube have same motion behaviour about an equatorial plane (i.e. the plane that divides the tube into two equal halves). Besides analysing the physical model, we have carried out numerical simulation of the model based on an idealized structural analysis with fold stiffness as $K_f = 1 \times 10^{-1} \text{ N}$ (refer to supplementary material SM2 for detailed description). The structural analysis is performed using an

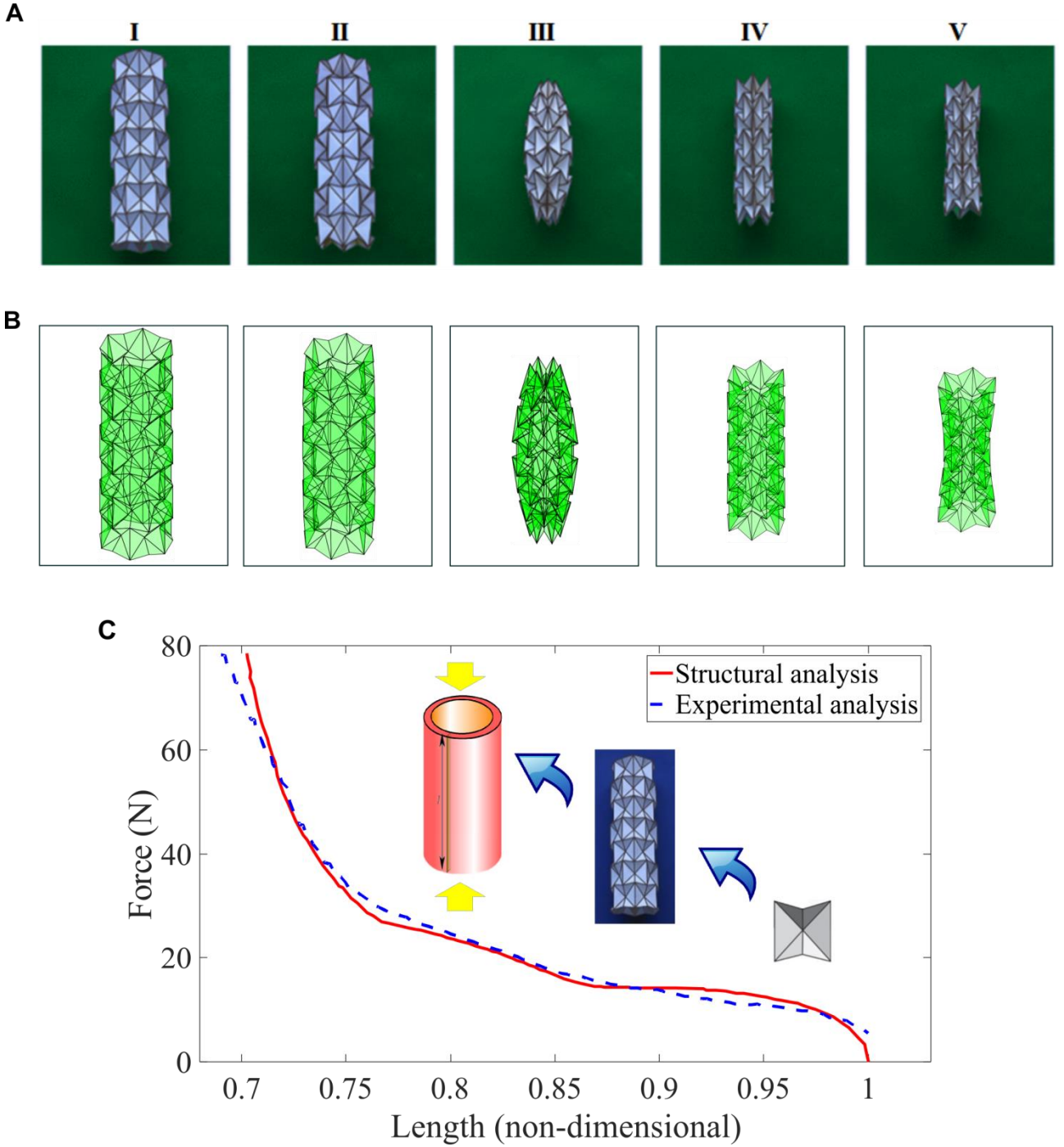


Figure 2. Deformation-dependent stiffness modulation feature in the tubular metamaterial. **A.** Physical model of a waterbomb tube under the application of axial compressive force from the expanded configuration to the fully contracted configuration (Configuration I to V) **B.** Simulated model of the waterbomb tube under application of a compressive force showing different stages of deformation (Non-dimensional lengths of the tube corresponding to the simulated stages are, Configuration I: 1; Configuration II: 0.97; Configuration III: 0.79 (point of first contact); Configuration IV: 0.73; Configuration V: 0.71) **C.** Force vs. length (deformation) curve with comparative results among structural and experimental analyses. Here the length of the tube is non-dimensionalized with respect to the initial length (The geometry of the tube was selected as follows: $n=6$, $m=7$, $\alpha=45^\circ$, $a=22.5\text{mm}$, and an initial dihedral angle $\theta=144^\circ$ which corresponded to a uniform radius configuration).

idealised bar, spring and hinge model of the origami structure [23, 24], a brief description of which is provided in supplementary material SM2 (an implementation of this analogy in MERLIN [25] is followed in this paper). The extent of structural response here is affected by fold stiffness and stiffness of the idealized bar depending on the stage of deformation. It is noted that the deformed shapes at different stages of deformation obtained using the structural simulation (Fig. 2B) are in good agreement qualitatively with that of the physical model (Fig. 2A), corroborating a high level of confidence in the current analysis. The model is further validated quantitatively using the constitutive relations in the following paragraphs.

Based on the microstructural geometric parameters discussed in the preceding paragraphs, we analyse different configurations of the waterbomb tube and discuss their stiffness, shape modulation and distant actuation characteristics here. To demonstrate the deformation-dependent stiffness, that can be predictively modelled as a function of the applied far-field load (or deformation), the constitutive relation of the waterbomb tube with $n = 6$, $m = 7$ and $\alpha = 45^\circ$ under longitudinal compression is shown in Fig. 2C following two different forms of analyses: structural and experimental investigations. The methodology followed for the longitudinal compression experiment is provided in supplementary material SM1, while the structural analysis (numerical) is described in supplementary material SM2. In these two forms of analysis, the tube starts from the configuration of a uniform radius throughout the length, and the length is presented as a non-dimensional ratio of deformed length and initial length of the tube. The initial uniform radius configuration can be selected based on a preliminary geometric analysis as presented in reference [26]. Here the axial reaction force is non-zero in the experimental model due to the rest angle of the folds and the structural model is unstressed at the initial configuration. The good agreement between the results of the numerical and experimental studies presented in Fig. 2C corroborates the validity of the subsequent analyses presented in this paper.

The constitutive curve of Fig. 2C shows a substantial increase in the stiffness during the deformation process when non-dimensional length of the tube becomes 0.79. Interestingly, this is the point where pure rigid origami motion ceases and the structural deformation sets in due to contact among the vertices of the waterbomb units. Thus, behavior of the proposed tubular origami metamaterial is not purely rigid; rather it shows a mixed mode (rigid and non-rigid) behavior. Initially under far-field actuation, the metamaterial undergoes a purely rigid deformation (i.e. deformation due to folding along the creases only) until contact among the vertices occurs. After this point, the tube becomes an enclosed volume. Further shortening of the tube under axial compression by folding along creases alone without deforming the facets is impossible due to Connelly's conjecture [27]. At this stage, the facets also have to deform to allow any further longitudinal deformation of the tube. Therefore, a non-rigid behavior is observed in the post-contact

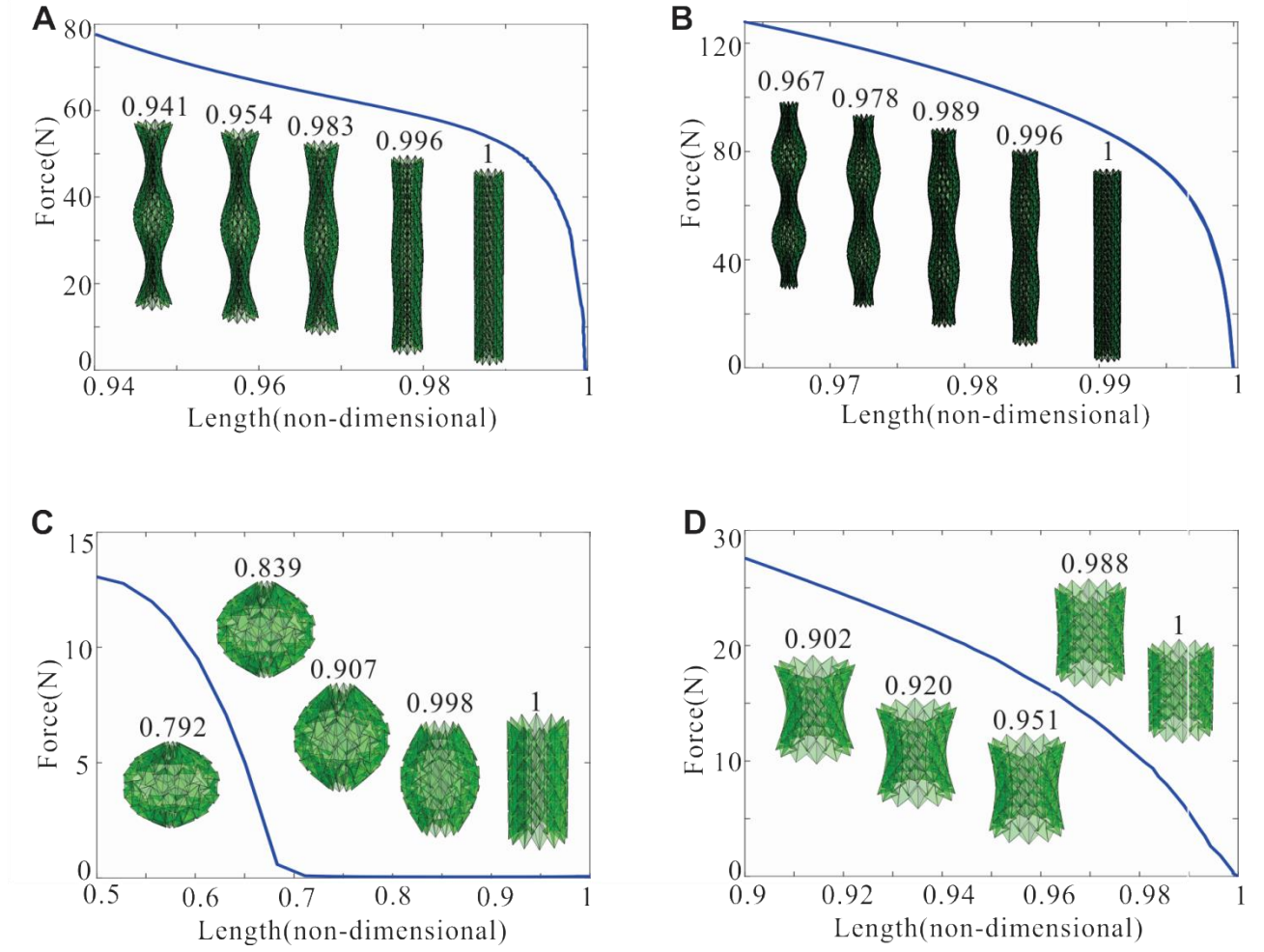


Figure 3. Programmable distant actuation feature in the tubular origami metamaterial. **A.** Constitutive relationship and microstructure-dependent motion behaviour for origami metamaterials with $m=25$, $n=12$ and $\alpha=46.83^\circ$. **B.** Constitutive relationship and microstructure-dependent motion behaviour for an origami metamaterial with $m=31$, $n=12$ and $\alpha=46.83^\circ$. **C.** Constitutive relationship and microstructure-dependent motion behaviour for an origami metamaterial with $m=7$, $n=12$ and $\alpha=46.83^\circ$. **D.** Constitutive relationship and microstructure-dependent motion behaviour for an origami metamaterial with $m=7$, $n=12$ and $\alpha=50.44^\circ$.

regime. After the occurrence of first contact, the load can still be transmitted through the equivalent bar-hinge-spring system beyond the points of contact along longitudinal direction of the tube. Thus, afterwards (post-contact) a mixed mode of deformation occurs involving both structural deformation and folding along creases. It can be noted here that this critical point of first contact is dependent on both the geometric parameters of the tube as well as the stiffness of the creases and facets. Thus, the steep increase in stiffness of the metamaterial can be designed as a function of deformation (or applied end-force) according to the application-specific requirement of a particular system. It is generally accepted in the field of metamaterials that variable stiffness can be obtained in a structural system as to where in the structure the stiffness is needed using a graded microstructural geometry. By introducing the proposed metamaterial, we show that it is now

possible to achieve variable stiffness as to when in the deformation process it is needed. The aspect of achieving extreme stiffness values in the system as a function of applied far-field force (/end deformation) is illustrated further in the later part of this article. [In this context it can be noted that variable stiffness in origami metamaterial was previously shown using a self-locking mechanism \[28\].](#)

After probing the behaviour of a waterbomb tube with $n = 6$, $m = 7$ and $\alpha = 45^\circ$ along with establishing the constitutive relations based on two different forms of analyses, we have investigated the waterbomb based tubular metamaterial in more depth considering different other values of n and m . The waterbomb tube reveals various interesting spatial profiles when an increased number of waterbomb bases is considered in a row ($n = 12$). Fig. 3A and 3B show the constitutive relationship between force and non-dimensional length of the tubes with $m = 25$ and $m = 31$ respectively ($\alpha = 46.83^\circ$). The spatial profile of the tubes show the formation of waves where some portion of the tube bulge radially outward while the remaining portions shrink in a radially inward direction. The number of bulges increase from one to two for the two configurations corresponding to $m = 25$ and $m = 31$. The radius of the tube expands near the edges for the configuration with $m = 25$, while a reverse trend is noticed in the case of $m = 31$. When a smaller number of rows is considered with $m = 7$, $n = 12$, and $\alpha = 46.83^\circ$ (Fig. 3C), a single convex surface is formed. The nature of the surface curvature can be reversed to concave by considering a higher value of α , e.g., $\alpha = 50.44^\circ$, as shown in Fig. 3D. The mechanical behaviour of short-length and large-diameter tubular metamaterials are further presented in supplementary material SM3 (refer to figures S3 and S4). The micro-structure dependent shape modulation of the origami metamaterials are further demonstrated in supplementary video SV1 – SV5. [It can be noted here that the behaviour of the origami tubes may have an analogy to the local buckling modes in a thin-walled cylinder, transitioning from a pure axial compression to a response dominated by bending.](#) The results presented in Fig. 3 show that [nature and degree of the local waviness on the surface of the tubular origami structure can be distantly activated and controlled by a far-field load without the need of installing any embedded local spatial sensors, actuators and controllers, effectively leading to a programmable *shape modulation and distant actuation feature*.](#) It can be noted that an inverse identification approach based on optimization could be adopted to design microstructures for achieving a desired spatial profile. Further the controllable spatial profile of the tubular metamaterials leads to a unique deformation dependent spatially varying Poisson's ratio (positive, negative [29] and a mixed mode behaviour), which is achievable from a uniform initial microstructural configuration (previous papers show that spatially varying Poisson's ratio can be achieved from non-uniform microstructures [30]) of the metamaterial (refer to supplementary

material SM4 for detailed description). A programable mixed auxetic and non-auxetic behaviour can be obtained in a single configuration of the tubular metamaterial.

In addition to the shape modulation and distant actuation feature, it is interesting to note the constitutive relationship in Fig. 3C, where significant amount of deformation can be achieved with negligible increase in the applied force up to a point with critical non-dimensional length of the tube $L_{cr} = 0.6831$ (the corresponding force at the critical point is recorded as 0.056N). Thus, we are able to obtain a *mechanism-like behaviour* (i.e. near-zero stiffness) up to L_{cr} by appropriately designing the micro-structure of the tubular metamaterial, wherein a definite amount of external energy is required for the system to deform. It can be noted in this context that perfectly *zero-stiffness* response in an elastic structure is only possible when strain energy gets redistributed within the structure i.e. there should be a balance between the energy released from negative stiffness and absorbed by positive stiffness. However, the current structure shows a ‘near-zero’ stiffness, not perfectly zero stiffness. Slope of the curve in the region of 1 to L_{cr} is not perfectly zero, but positive and close to zero. Very small amount of force increment is required in this region for axial deformation of the tube to occur. Thus, stiffness of the structure in this region is not perfectly zero, but it is much less compared to the high stiffness beyond L_{cr} .

We have verified the energy conservation of the system by noting that total externally applied energy (external far-field load multiplied by deformation) is equal to the sum of energy required due to rotation (opening and closing) of all the folds in the system. Having the energy conservation principle satisfied, we can further explain the behaviour in terms of force equilibrium to elucidate the possible reason for the requirement of very small amount of force increment for axial deformation of the tube until the critical length L_{cr} . During compressive motion of the tube, some of the constituting folds open up, while others tend to close. The two opposite motion behaviours of the folds would require forces of two opposite nature to be applied to the respective folds. Here the components of the relatively opposite forces are adjusted along the axial direction of the tube in such a way that negligible external force increment is required for the tube to undergo compressive deformation until L_{cr} . Thus, the behaviour of the tube is consistent from both energy conservation and force equilibrium point of view.

Some of the vertices come in contact with each other after the critical point (L_{cr}), leading to a significant increase in stiffness and subsequent increase in the far-field force. Besides the shape modulation and distant actuation features, it is evident from the above discussion that the proposed origami metamaterial, depending on its microstructural configuration, is able to achieve extreme level of deformation-dependent programmable stiffness modulation ranging from a near-zero stiffness (non-dimensional length $> L_{cr}$) to a very high value of stiffness (non-dimensional length $<$

L_{cr}). More interestingly, the extreme stiffness modulation in the system being dependent on far-field force (/deformation), the desired extreme values are achievable when in the deformation process they are needed according to application-specific requirements.

In the proposed origami-based metamaterial, either a displacement or a force can be applied at the two ends to program the material. This external displacement/ force is referred here as ‘distant actuation’. The word ‘distant’ is used because the action of the applied force/ displacement at the ends of the tubular metamaterial can result in a change in its shape far away from the point of actuation. As a result of this external far-field actuation, local shape modulation can be achieved based on the microstructural configuration of the origami tube as per the requirement of a specific application. In this context it can be noted that shape morphing was hinted by means of buckling in textured materials in previous studies [31].

In addition to shape, stiffness of the system can also be programmed as a function of the extent of far-field actuation. It is worthy to note that the transition of rigid body motion to structural deformation under the application of far-field actuation allows us to design programmable stiffness in the proposed tubular metamaterial. This transition takes place when the internal vertices of the tubular metamaterial come in contact. Essentially, after this point the tubular metamaterial must undergo structural deformation to allow a net far-field axial movement of the points of actuation. Since the stiffness in case of structural deformation is much more than the stiffness of an origami fold, a sudden and sharp rise in stiffness can be programmed based on the point when this transition occurs in the deformation process. The point of transition can be modulated as a function of the microstructural configuration of the system. In case of cellular metamaterials based on lattices [1, 2], as there is no such possibility of having mixed mode deformation with a transition point, the possibility of programming stiffness to have sudden and sharp rise in its value does not normally arise. In summary, the programable shape and stiffness of the proposed tubular metamaterial can be designed depending on the microstructural configuration and the extent of applied far-field actuation.

3. Discussion

Through combined numerical and experimental analyses we have developed a novel material microstructure by uncovering the programmable deformation-dependent stiffness, and shape modulation-dependent distant actuation characteristics of waterbomb based tubular origami metamaterial along with its dependency on the geometrical parameters and assembly of the base pattern. The tubular metamaterial can exhibit a unique spatially varying Poisson’s ratio (positive, negative and a mixed mode behaviour), which is achievable from a uniform initial configuration of the metamaterial. We have shown that the stiffness of the tubular metamaterial can be modulated as

a function of the applied far-field deformation (/force) along with the geometric configurations and material attributes. A near-zero value as well as an extreme rise in stiffness can also be programmed according to application-specific requirements. Thus, we essentially develop a metamaterial here, wherein besides being able to assign the stiffness as to where in a structure it is needed (using spatially varying graded microstructure), it is also possible to achieve variable stiffness (including extreme values) as to when in the deformation process it is needed. This will lead to the development of ultimate lightweight multifunctional structural systems where the stiffness can be most optimally utilized.

We have revealed that the local shape (both the nature and degree of waviness) of the tubular metamaterial can be distantly activated and controlled by a far-field load. Here it is noteworthy that the spatial shape modulation is achievable from an initial uniform configuration, contrary to the behaviour of conventional materials. The distant actuation feature reveals a rational approach to develop functional materials that can be programmed for specific local deformations in the metamaterial without installing any complex network of local embedded sensors, actuators and controllers. These intriguing properties make the proposed tubular origami metamaterial an ideal candidate for creation of innovative programmable metamaterials with various functional features that can serve as a catalyst for the uptake of this origami object in wide range of applications such as mechanical and aerospace systems, soft robotics, morphing structures, and medical devices.

Materials and methods

Fabrication of prototypes

The physical model shown in Fig. 2A was made from conventional cards for understanding the behavior of the origami tube. To investigate the longitudinal stiffness of the waterbomb tube, a specimen made from PP sheet of 0.34mm in thickness was constructed and compressed in the longitudinal direction. The geometry of the tube was selected as follows: $n = 6$, $m = 7$, $\alpha = 45^\circ$, $a = 22.5\text{mm}$, and an initial dihedral angle $\theta = 144^\circ$ which corresponded to a uniform radius configuration. The crease lines were created by laser cutting (Trotec Speedy 300) and then folded by hands to form the tube. In addition, ENDURO Ice sheets with 0.29mm in thickness were used to reinforce the panels so as to generate a rigid folding motion, i.e., only the creases rotate whilst the panels remain undeformed. Detail description of the experiment methodology is provided in the supplementary material.

Structural analysis method

Detail description about the structural analysis method followed in this work is provided in the supplementary material.

Supplementary materials

Supplementary Text

Figures: S1 to S5.

Movies: Movie SV1 – Animation of Fig. 3A

Movie SV2 – Animation of Fig. 3B

Movie SV3 – Animation of Fig. 3C

Movie SV4 – Animation of Fig. 3D

Movie SV5 – Animation of Fig. S4

Acknowledgments

T. M. and Z. Y. acknowledges the support of the Air Force Office of Scientific Research (FA9550-16-1-0339), Y. C. acknowledges the support of the National Natural Science Foundation of China (Projects 51825503 and 51721003), and J. M. acknowledges the support of the National Natural Science Foundation of China (Project 51575377).

Data availability

All data used to generate these results is available in the main text or supplementary material. Further details could be obtained from the corresponding authors upon request.

References

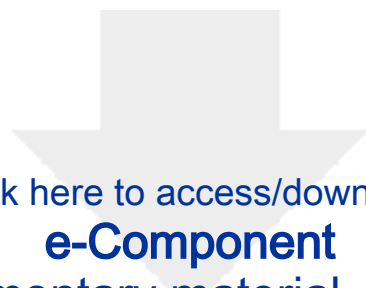
1. X. Zheng, H. Lee, T. H. Weisgraber, M. Shusteff, J. DeOtte, E. B. Duoss, J. D. Kuntz, M. M. Biener, Q. Ge, J. A. Jackson, S. O. Kucheyev, N. X. Fang, C. M. Spadaccini, Ultralight, ultrastiff mechanical metamaterials. *Science*, 344(6190), 1373-1377 (2014).
2. T. Mukhopadhyay, S. Adhikari, Stochastic mechanics of metamaterials, *Composite Structures*, 162 85–97 (2017)
3. C. Zschoernack, M. A. Wadee, C. Völlmecke, Nonlinear buckling of fibre-reinforced unit cells of lattice materials, *Composite Structures*, 136 217-228 (2016)
4. S. J. P. Callens, N. Tümer, A. A. Zadpoor, Hyperbolic origami-inspired folding of triply periodic minimal surface structures, *Applied Materials Today*, 15 453-461 (2019)
5. L.R. Meza, G.P. Phlipot, C.M. Portela, A. Maggi, L.C. Montemayor, A. Comella, D.M. Kochmann, J.R. Greer, Reexamining the mechanical property space of three-dimensional lattice architectures, *Acta Materialia*, 140 424-432 (2017)
6. Z. Y. Wei, Z. V. Guo, L. Dudte, H. Y. Liang, L. Mahadevan, Geometric mechanics of periodic pleated origami. *Phys. Rev. Lett.* 110, 215501 (2013).
7. M. Schenk, S. D. Guest, Geometry of Miura-folded metamaterials. *Proc. Natl Acad. Sci. USA* 110, 3276-3281 (2013).
8. E. T. Filipov, T. Tachi, & G. H. Paulino, Origami tubes assembled into stiff, yet reconfigurable structures and metamaterials. *Proceedings of the National Academy of Sciences*, 112(40), 12321-12326 (2015)
9. J. L. Silverberg, et al. Origami structures with a critical transition to bistability arising from hidden degrees of freedom. *Nature Mater.* 14, 389-393 (2015).

10. J. L. Silverberg, et al. Using origami design principles to fold reprogrammable mechanical metamaterials. *Science* 345, 647-650 (2014).
11. S. Waitukaitis, R. Menaut, B. Chen, M. van Hecke, Origami multistability: from single vertices to metasheets. *Phys. Rev. Lett.* 114, 055503 (2015).
12. L. Fan , H. Ge, S. Y. Zhang, H. Zhang, Research on pass band with negative phase velocity in tubular acoustic metamaterial. *Journal of Applied Physics*, 112(5), 053523 (2012)
13. H. Yasuda, T. Tachi, M. Lee, J. Yang, Origami-based tunable truss structures for non-volatile mechanical memory operation, *Nature communications*, 8(1), 962 (2017)
14. Z. Zhai, Y. Wang, H. Jiang , Origami-inspired, on-demand deployable and collapsible mechanical metamaterials with tunable stiffness, *Proceedings of the National Academy of Sciences*, doi.org/10.1073/pnas.1720171115
15. S. Randlett, *The Art of Origami*. (Faber & Faber, 1961).
16. S. Fujimoto, M. Nishiwaki, An invitation to creative origami play, in *Osaka, Japan, Asahi Culture Centre* (In Japanese, 1982).
17. B. Kresling, Plant "design": mechanical simulations of growth patterns and bionics. *Biomimetics*. 3, 105-122 (1995).
18. Y. Chen, H. Feng, J. Ma, R. Peng, Z. You, Symmetric waterbomb origami, *Proc. R. Soc. A* 472: 20150846 (2016).
19. K. Kuribayashi, Z. You, Expandable tubes with negative Poisson's ratio and their applications in medicine, in *Origami⁵: Fourth International Meeting of Origami Science, Mathematics, and Education*, 117-128 (A K Peters, 2009).
20. K. Kuribayashi, et al. Self-deployable origami stent grafts as a biomedical application of Ni-rich TiNi shape memory alloy foil. *Materials Science and Engineering: A* 419, 131-137 (2006).
21. C. D. Onal , R. J. Wood, D. Rus, An origami-inspired approach to worm robots. *Mechatronics, IEEE/ASME Transactions* 18, 430-438 (2013).
22. D.-Y. Lee, et al. The deformable wheel robot using magic-ball origami structure, in *IDETC/CIE* (2013).
23. K. Liu, G. H. Paulino, Nonlinear mechanics of non-rigid origami: an efficient computational approach. *Proc. R. Soc. A*, 473(2206), 20170348 (2017)
24. M. Schenk, S. D. Guest, Origami folding: a structural engineering approach. In *Origami 5* (eds P Wang-Iverson, RJ Lang, M Yim), pp. 293–305. Boca Raton, FL: CRC Press (2011)
25. K. Liu, G. H. Paulino. MERLIN: A MATLAB implementation to capture highly nonlinear behavior of non-rigid origami. In *Proc. of the IASS Annual Symp; Spatial Structures in the 21st century*, Tokyo, Japan, 26–28 September, 2016 (eds K. Kawaguchi, M. Ohsaki, T. Takeuchi). Madrid, Spain: IASS
26. J. Ma, Z. You. Modelling of the waterbomb origami pattern and its applications. In *ASME 2014 International Design Engineering Technical Conferences and Computers and Information in Engineering Conference* (pp. V05BT08A047-V05BT08A047). *American Society of Mechanical Engineers*, (2014)

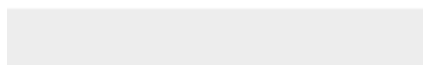
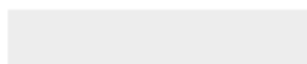
27. R. Connelly, I. Sabitov, A. Walz, The Bellows Conjecture, *Contrib. Algebra Geom.* 38 1-10, (1997)
28. H. Fang, S. C. A. Chu, Y. Xia, K. W. Wang, Programmable Self-Locking Origami Mechanical Metamaterials. *Advanced Materials*, 30(15), 1706311 (2018)
29. J.N. Grima, L. Mizzi, K.M. Azzopardi, R. Gatt, Auxetic perforated mechanical metamaterials with randomly oriented cuts, *Advanced Materials*, 28 (2) 385-389 (2016)
30. R. Hedayati, M. J. Mirzaali, L. Vergani, A. A. Zadpoor, Action-at-a-distance metamaterials: Distributed local actuation through far-field global forces. *APL Materials*, 6(3), 036101 (2018)
31. K. A. Seffen, S. V. Stott Surface texturing through cylinder buckling. *Journal of Applied Mechanics*, 81(6), 061001 (2014)

Conflict of interest statement

The authors declare no conflict of interest.



Click here to access/download
e-Component
Supplementary material_AMT.pdf







[Click here to access/download](#)

Video
SV2.mp4







[Click here to access/download](#)

Video

SV4.mp4





[Click here to access/download](#)

Video

SV5.mp4

